

Complexity in parametric Bose-Hubbard Hamiltonians and structural analysis of eigenstates

Moritz Hiller,^{1,2,3} Tsampikos Kottos,^{1,2} and T. Geisel^{2,3}

¹*Department of Physics, Wesleyan University, Middletown, Connecticut 06459, USA*

²*MPI for Dynamics and Self-Organization, Bunsenstr a e 10, D-37073 G ttingen, Germany*

³*Fakult t f r Physik, Universit t G ttingen, Friedrich-Hund-Platz 1, D-37077 G ttingen, Germany*

We consider a family of chaotic Bose-Hubbard Hamiltonians (BHH) parameterized by the coupling strength k between neighboring sites. As k increases the eigenstates undergo changes, reflected in the structure of the Local Density of States. We analyze these changes, both numerically and analytically, using perturbative and semiclassical methods. Although our focus is on the quantum trimer, the presented methodology is applicable for the analysis of longer lattices as well.

PACS numbers: 34.30.+h, 05.30.Jp, 03.75.Lm

Understanding the complicated behavior of quantum many-body systems of interacting Bosons has been a major challenge for leading research groups over the last few years. In fact, the growing theoretical interest was further enhanced by recent experimental achievements. The most fascinating of these was the realization of Bose-Einstein condensation (BEC) of ultra-cold atoms in periodic optical lattices [1], which allows for novel concrete applications of quantum mechanics such as atom interferometers and atom lasers. The flood of experimental realizations includes systems ranging from bond-excitations in molecules [2] to cantilever vibrations in micro-mechanical arrays [3] and Josephson arrays [4].

The simplest non-trivial model that describes interacting bosons on a lattice is the Bose-Hubbard Hamiltonian (BHH), which incorporates the competition between kinetic and interaction energy of the bosonic system. In a substantial part of the existing literature (see for example [5]), the dynamics and spectral properties of BHH was investigated using a semiclassical picture. In contrast, quantum mechanical calculations of a BHH are often limited by severe computational memory restrictions. However, it is possible to treat small systems with two or three lattice sites. These studies are extremely relevant to bond excitations in small molecules [6], few coupled Josephson junctions and BECs in optical traps with just a few wells [7]. As to the experimental realization of the last case, microtrap technology [8] is probably the most promising approach for realizing these small systems. Remarkably, there is already an experimental realization [9], with promising applications.

In this context, the two-site system (dimer) has been analyzed thoroughly from both the semiclassical [10, 11] and the purely quantum viewpoint [5, 12, 13]. Such investigations have revealed many interesting phenomena like the onset of π -phase oscillations, symmetry-breaking, and self-trapping of boson population, the latter being observed experimentally in [9]. In fact, the dimer is integrable since there are two conserved quantities, the energy and the number of bosons. Nevertheless, the richness of the results provides a motivation to go beyond the dimer and consider new scenarios where even richer

dynamics should be observed. The trimer opens new exciting opportunities, in this respect, since the addition of a third site leads to (classically) chaotic behavior, thus paving the way to understand longer lattices. The trimer has been studied quite extensively in the semiclassical regime [14, 15, 16]. Surprisingly enough, the quantum trimer [17, 18] (not to mention longer lattices [19]) is barely treated. As a matter of fact, the majority of the quantum studies are focused on the statistical properties of levels [17]. However, spectral statistics is only the first step in understanding the behavior of a complex quantum system. Substantially more insight is gained through the study of eigenstates.

In this paper we consider the quantum trimer in the chaotic regime and study the structural changes that the eigenstates undergo as an experimentally controlled parameter k (the coupling strength between neighboring sites) is varied. The object of our interest is the overlap of a given perturbed eigenstate $|n(k_0 + \delta k)\rangle$ with the eigenstates $|m(k_0)\rangle$ of the unperturbed trimer

$$P(n|m) = |\langle n(k_0 + \delta k)|m(k_0)\rangle|^2. \quad (1)$$

Alternatively, if regarded as a function of n for a fixed m , the kernel $P(n|m)$ represents (up to some trivial scaling) the Local Density of States (LDoS) [20]. Its lineshape is fundamental for the understanding of the associated dynamics since its Fourier transform is the so-called ‘‘survival probability amplitude’’. In our studies, we have identified three structural regimes of the $P(n|m)$, which are associated with two parametric scales defined as

$$\delta k_{\text{qm}} \propto \tilde{U}/N^{3/2} \quad \text{and} \quad \delta k_{\text{prt}} \propto \tilde{U}/N, \quad (2)$$

where $\tilde{U} = NU$, N is the number of interacting bosons and U is the on-site boson-boson interaction. For $\delta k < \delta k_{\text{qm}}$ the perturbation mixes only neighboring levels: the main component of the kernel $P(n|m)$ remains unaffected while corrections are captured by standard textbook finite order perturbation theory. For $\delta k_{\text{qm}} < \delta k < \delta k_{\text{prt}}$ a non-trivial structure appears, consisting of two distinct components: while the tails are still captured by perturbation theory, the central part is of non-perturbative

nature and extends over an energy width $\Gamma \propto N^2 \cdot \delta k^2 / \tilde{U}$. For $\delta k > \delta k_{\text{prt}}$, quantum mechanical perturbation theory fails totally. Instead, classical calculations can be used to predict the shape of $P(n|m)$. An overview of the parametric evolution of $P(n|m)$ is shown in Fig. 1.

The trimeric Bose-Hubbard-Hamiltonian, which describes an interacting boson gas confined in a three well lattice, is given in second quantization by:

$$\hat{H} = 0.5U \sum_{i=1}^3 \hat{n}_i(\hat{n}_i - 1) - k \sum_{i \neq j} \hat{b}_i^\dagger \hat{b}_j; \quad \hbar = 1. \quad (3)$$

In the BEC framework, $k = k_0 + \delta k$, is the coupling strength between adjacent sites i, j , and can be controlled experimentally (in the context of optical lattices this can be achieved by adjusting the intensity of the laser beams that create the trimeric lattice), while $U = 4\pi\hbar^2 a_s V_{\text{eff}}/m$ describes the interaction between two atoms on a single site (V_{eff} is the effective mode volume of each site, m is the atomic mass, and a_s is the s -wave scattering length of atoms). In the context of molecular physics [2, 12] k represents the electromagnetic and mechanical coupling between the bonds of adjacent molecules i, j , while U represents the anharmonic softening of the bonds under extension. The operators $\hat{n}_i = \hat{b}_i^\dagger \hat{b}_i$ count the number of bosons at site i ; the annihilation and creation operators \hat{b}_i and \hat{b}_i^\dagger obey the canonical commutation relations $[\hat{b}_i, \hat{b}_j^\dagger] = \delta_{i,j}$. Hamiltonian (3) has two constants of motion, namely the energy E and the total number of particles $N = \sum_{i=1}^3 n_i$. Having $N = \text{const.}$ implies a finite Hilbert-space of dimension $\mathcal{N} = (N+2)(N+1)/2$ [12, 17]. An additional 3-fold permutation symmetry allows us to reduce further the dimensionality of our space [17].

When $N \gg 1$ one can adopt a semiclassical point of view for Hamiltonian (3). Formally, this can be seen if we define rescaled creation and annihilation operators $\hat{c}_i = 1/\sqrt{N} \hat{b}_i$. The corresponding commutators $[\hat{c}_i, \hat{c}_j^\dagger] = \delta_{ij}/N$ vanish for $N \gg 1$ and therefore one can treat the rescaled operators as c -numbers. The classical Hamiltonian H is obtained using the Heisenberg relations $\hat{c}_i \rightarrow \sqrt{I_i} \exp^{i\varphi_i}$ where φ_i is an angle and I_i is the associated action. We then get

$$\tilde{\mathcal{H}} = \frac{\mathcal{H}}{N\tilde{U}} = \frac{1}{2} \sum_{i=1}^3 I_i^2 - \lambda \sum_{i \neq j} \sqrt{I_i I_j} \exp^{i(\varphi_j - \varphi_i)}. \quad (4)$$

The dynamics is obtained from (4) using the canonical equations $dI_i/d\tilde{t} = -\partial\tilde{\mathcal{H}}/\partial\varphi_i$ and $d\varphi_i/d\tilde{t} = \partial\tilde{\mathcal{H}}/\partial I_i$. Here $\tilde{t} = \tilde{U} \cdot t$ is the rescaled time. The dimensionless ratio $\lambda \equiv k/\tilde{U}$ [6, 11, 15, 17, 18] determines the dynamics of the classical Hamiltonian (4). For $\lambda \rightarrow 0$ the interaction term dominates and the system behaves as a set of uncoupled sites while for $\lambda \rightarrow \infty$ the kinetic term is the dominant one. In both limits the motion is integrable. We consider intermediate values of λ where the classical dynamics is chaotic. The semiclassical limit is approached by keeping λ_0 and \tilde{U} constant while $N \rightarrow \infty$.

This is crucial in order to keep the underlying classical motion unaffected.

We assume that both $\tilde{\mathcal{H}}_0 = \tilde{\mathcal{H}}(\lambda_0)$ and $\tilde{\mathcal{H}} = \tilde{\mathcal{H}}(\lambda)$ generate classically chaotic dynamics of similar nature. This is equivalent with the requirement that $\delta\lambda \equiv (\lambda - \lambda_0)$ is *classically small*, i.e., $\delta\lambda \ll \delta\lambda_{\text{cl}}$. An important classical observable is the generalized force $\tilde{\mathcal{F}}(\tilde{t}) \equiv -(\partial\tilde{\mathcal{H}}/\partial\lambda) = \sum_{i \neq j} \sqrt{I_i I_j} \exp^{i(\varphi_j - \varphi_i)}$. Due to the chaotic dynamics the power spectrum $\tilde{C}(\tilde{\omega})$ has a finite support $\tilde{\Omega}_{\text{cl}} = 2\pi/\tilde{t}_{\text{erg}}$ with \tilde{t}_{erg} being the ergodic time of the system described by Eq. (4). One can use $\tilde{C}(\tilde{\omega})$ as an operative way to evaluate $\delta\lambda_{\text{cl}}$. The latter is the maximum perturbation which keeps $\tilde{C}(\tilde{\omega})$ unaffected. We note that in the experiment, the relevant parameter that is tuned is the coupling strength $\delta k_{\text{cl}} = \tilde{U} \cdot \delta\lambda_{\text{cl}}$. We have found that for $0.04 \leq \lambda \leq 0.2$ and in an energy interval $\tilde{H} \approx 0.26 \pm 0.02$ the motion is predominantly chaotic. In this regime, and for $\tilde{U} = 280$ we get $\delta k_{\text{cl}} = 20$ while $\tilde{\Omega}_{\text{cl}} \approx 1$ (see Fig. 2a).

Quantum mechanically, we work in the eigenbasis of the Hamiltonian \hat{H}_0 . In this basis \hat{H}_0 becomes diagonal i.e. $\mathbf{E}_0 = E_m^{(0)} \delta_{mn}$ where $\{E_m^{(0)}\}$ are the ordered eigenvalues. Their mean level spacing $\Delta \approx 1.5\tilde{U}/N$ can be estimated using $\mathcal{N} \propto N^2$ together with Eq. (4). The perturbed Hamiltonian \hat{H} is written as

$$\mathbf{H} = \mathbf{E}_0 - \delta k \mathbf{B} \quad (5)$$

We mark that although the perturbation strength δk is assumed to be classically small ($\delta k \leq \delta k_{\text{cl}}$), quantum-mechanically it can be very *large*, i.e., it can mix many levels (see the avoided crossings appearing in Fig. 1 for large values of δk). From exact diagonalization we find that \mathbf{B} is a *banded matrix*. Its bandprofile can be determined using a semiclassical recipe $\langle |\mathbf{B}_{nm}|^2 \rangle \approx (N^2/\tilde{U})\Delta \cdot \tilde{C}(\omega_{nm})/2\pi$ [21]. The bandwidth is $\Delta_b = \tilde{\Omega}_{\text{cl}} \cdot \tilde{U}$. It is common to define $b \equiv \Delta_b/\Delta \approx 0.6N$. The banded matrix \mathbf{B} and the band profile are illustrated in Fig. 2a.

A fixed assumption of this work is that $\delta k \ll \delta k_{\text{cl}}$. If we require the perturbation to be also *quantum mechanically small* $\delta k \leq \delta k_{\text{qm}}$, then we can apply standard first order perturbation theory (FOPT) (see Fig. 2b). In this case $P_{\text{FOPT}}(n|m) \approx 1$ for $n = m$, while $P_{\text{FOPT}}(n|m) = \delta k^2 \langle |\mathbf{B}_{nm}|^2 \rangle / (E_n - E_m)^2$. The perturbation strength δk_{qm} is given by the condition that only neighboring levels are mixed, yielding $\delta k_{\text{qm}} = \Delta/\sqrt{\langle |\mathbf{B}_{nm}|^2 \rangle}$. Substituting the expressions for Δ and $\langle |\mathbf{B}_{nm}|^2 \rangle$ we obtain the results reported in Eq. (2). In Fig. 3 we report our numerical results for δk_{qm} [22]. A nice agreement with Eq. (2) is observed.

For stronger perturbations $\delta k_{\text{qm}} < \delta k$ one has to employ perturbation theory to infinite order. Until now, the only formal results regarding Hamiltonians of the type (5), have been derived by Wigner [23]. He assumed that \mathbf{B}_{nm} is a *Banded Random Matrix* with a flat band profile and found that $P(n|m)$ is a Lorentzian

$$P_{\text{prt}}(n|m) = \frac{\delta k^2 |\mathbf{B}_{nm}|^2}{\Gamma^2 + (E_n - E_m)^2}, \quad \Gamma = \frac{\langle |\mathbf{B}_{nm}|^2 \rangle}{\Delta} \delta k^2. \quad (6)$$

For $\Gamma \leq \Delta$ Eq. (6) reduces to P_{FOPT} while for $\Delta < \Gamma < \Delta_b$ the kernel $P(n|m)$ contains two distinct components: a central region $|E_n - E_m| \leq \Gamma$ where the mixing of levels is non-perturbative and a tail region $\Gamma < |E_n - E_m| < \Delta_b$ which can still be captured by perturbation theory. The condition $\Gamma \sim \Delta_b$ determines δk_{prt} above which the non-perturbative core extends all over the bandwidth. Therefore (6) applies as long as $\delta k < \delta k_{\text{prt}} \propto \delta k_{\text{qm}} \cdot b^{0.5}$. In the case of non-interacting systems with chaotic classical limit recent studies [24, 25] indicated that the above scenario, based on random matrix modeling, leads to a fairly good description of the kernel. Specifically, $P(n|m)$ was found to exhibit a core-tail structure where the width of the core scaled as $\Gamma \sim \delta k^\alpha$ with $1 < \alpha \leq 2$ [24] in contrast to Eq. (6). In these studies the parameter Γ was determined (for a given δk) by imposing normalization of $P_{\text{prt}}(n|m)$. We note that a strict Lorentzian is an idealization of the random matrix modeling.

Does our BHH model follow the same scenario or will the interactions affect the shape of $P(n|m)$? Already from Fig. 1 we see that as $\delta k > \delta k_{\text{qm}}$, a non-perturbative core starts to evolve and eventually spills over the whole bandwidth Δ_b . A more detailed comparison (see Fig. 2) between $P(n|m)$ and Eq. (6) shows an excellent agreement. In the inset of Fig. 3 we report the measured width Γ as a function of δk . Our numerical data are in agreement with a power law behavior $\Gamma \propto \delta k^\alpha$ with $\alpha = 2 \pm 0.01$. We then investigated the scaling behavior of δk_{prt} [22]. Our numerical data are reported in Fig. 3 and are in agreement with the results stated in Eq. (2). The latter equation can now be understood in the light of Wigner's arguments since $\delta k_{\text{prt}} \propto \delta k_{\text{qm}} \times b^{0.5}$ and $b \sim N$.

For $\delta k > \delta k_{\text{prt}}$ the core spills over the bandwidth and therefore perturbation theory, even to infinite order, is inapplicable for evaluating $P(n|m)$. In such cases one has to rely on completely non-perturbative methods [24, 25]. For the Wigner model, it was found that $P(n|m) = 1/(2\pi\Delta)\sqrt{4 - ((E_n - E_m)/\Delta)^2}$ [23] while in systems that have a semiclassical limit the overlap kernel becomes $P(n|m) = \text{tr}(\rho_n \rho_m)$. Here $\rho_m(\{I_i\}, \{\varphi_i\})$ and $\rho_n(\{I_i\}, \{\varphi_i\})$ are the Wigner functions that correspond to the eigenstates $|m(k_0)\rangle$ and $|n(k)\rangle$ respectively. The trace stands for $d\{I_i\}d\{\varphi_i\}/(2\pi\hbar)^d$ integration. In the classical limit ρ can be approximated by the corresponding micro-canonical distribution $\rho \propto \delta(E - \mathcal{H}(\{I_i\}, \{\varphi_i\}))$. The latter can be evaluated by projecting the dynamics generated by $\mathcal{H}_0(\{I_i\}, \{\varphi_i\}) = E_0$ onto the Hamiltonian $\mathcal{H}(\{I_i\}, \{\varphi_i\}) = E(t)$. In Fig. 4a we plot the resulting $E(t)$ as a function of time. The classical distribution $P(n|m)$ is constructed (Fig. 4b) from $E(t)$, averaged over a sufficiently long time.

In conclusion, we have analyzed the structural changes which the eigenstates of a trimeric BHH undergo as the

coupling strength δk between the neighboring sites is varied. We have found that for $\delta k < \delta k_{\text{prt}}$ perturbation theory (to infinite order if $\delta k > \delta k_{\text{qm}}$) is applicable. In this case, the power spectrum of the generalized force $\tilde{C}(\tilde{\omega})$ is an important ingredient for the the-

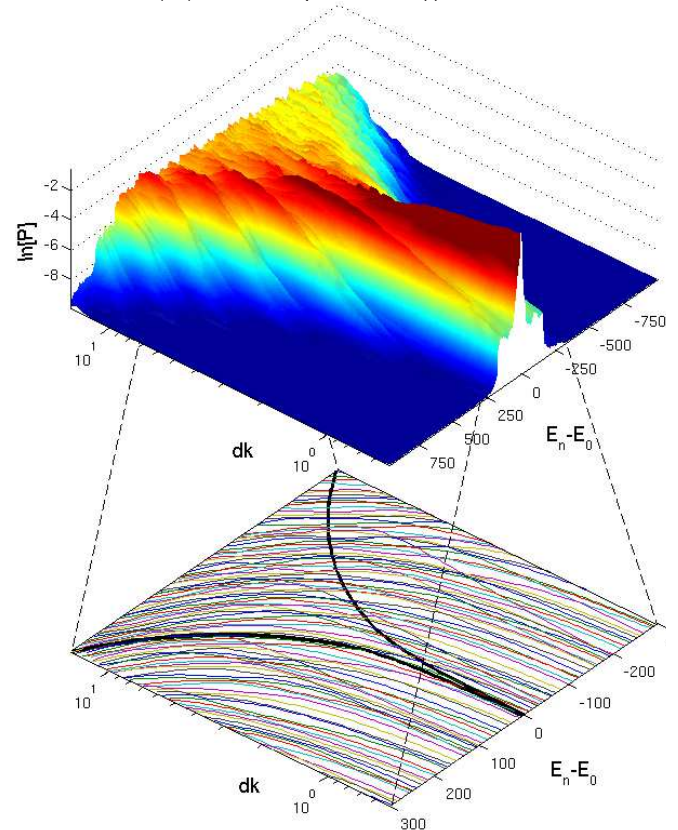


FIG. 1: (Color online) The kernel $P(n|m)$ of the BHH plotted as a function of the perturbed energies E_n (LDoS representation) and for various perturbation strengths $\delta k > \delta k_{\text{qm}}$. In the lower plane we report the parametric evolution of the energy levels within the bandwidth $\Delta_b \approx 230$. The energy width Γ is shown (bold line) as a function of δk . The averaged shape of eigenfunctions is given by the same kernel $P(n|m)$ and is obtained by just inverting the energy axis. Here, $N = 70$, and $\lambda_0 = 0.053$.

ory. It is directly experimentally measurable [26] because the momentum distribution of atoms in a lattice is $\sim \sum_j \exp(ikj)X_j$ where k is the atomic momentum and $X_j = \langle [\hat{b}_{j+l}^\dagger \hat{b}_l + \text{h.c.}] \rangle$ is the one-particle density matrix. In the opposite limit $\delta k > \delta k_{\text{prt}}$ one can apply semiclassical (non-perturbative) considerations.

It is our pleasure to acknowledge very fruitful discussions with D. Cohen and G. Kalosakas.

[1] M. Greiner *et al.*, Nature **415**, 39 (2002); D. Jaksch *et al.*, Phys. Rev. Lett. **81**, 3108 (1998).

[2] M. Joyeux *et al.*, Adv. Chem. Phys. **130**, 267 (2005); K.

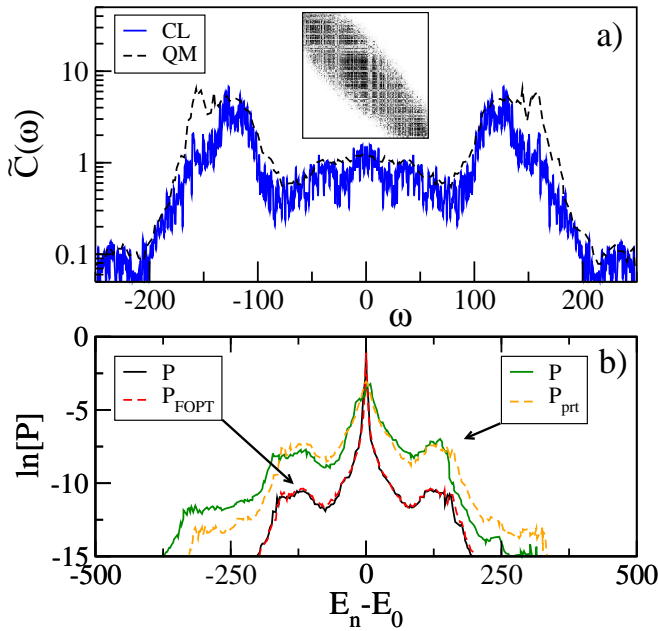


FIG. 2: (Color online) *Upper panel:* Comparison of the quantum band profile $\langle |B_{nm}|^2 \rangle (2\pi\tilde{U}/N^2\Delta)$ with the classical power spectrum $\tilde{C}(\omega)$. The number of particles is $N = 230$ and $\lambda_0 = 0.053$. The inset shows a snapshot of the matrix \mathbf{B} . *Lower panel:* The kernel $P(n|m)$ of the BHH (see Eq.(1)) for $\delta k = 0.05$ and for $\delta k = 0.3$ compared to the corresponding theoretical expressions P_{FOPT} and P_{prt} . Here $\delta k_{\text{qm}} = 0.09$ and $\delta k_{\text{prt}} = 1.02$.

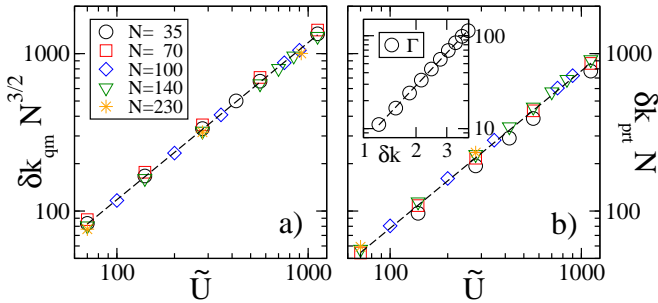


FIG. 3: (Color online) The parameters (a) δk_{qm} and (b) δk_{prt} for various \tilde{U}, N and for $\lambda_0 = 0.053$. A nice scaling in accordance with Eq.(2) is observed. In the inset of (b) we report the scaling of the energy width Γ with δk . The dashed line has slope 2.

- Lehmann, *et al.*, *Annu. Rev. Phys. Chem.* **45**, 241 (1994).
 [3] M. Sato *et al.*, *Phys. Rev. Lett.* **90**, 044102 (2003).
 [4] E. Trías, J. J. Mazo, and T. P. Orlando, *Phys. Rev. Lett.* **84**, 741 (2000); P. Binder *et al.*, *ibid.* **84**, 745 (2000).
 [5] R. Franzosi, V. Penna and R. Zecchina, *Int. J. Mod. Phys. B* **14**, 943 (2000).
 [6] A. C. Scott, P. S. Lomdahl, J. C. Eilbeck, *Chem. Phys. Lett.* **113**, 29 (1985); A. C. Scott, J. C. Eilbeck, *Chem. Phys. Lett.* **132**, 23 (1986); A. C. Scott, L. Bernstein, J. C. Eilbeck, *J. Biol. Phys.* **17**, 1 (1989).
 [7] A. Smerzi *et al.*, *Phys. Rev. Lett.* **79**, 4950 (1997); S.

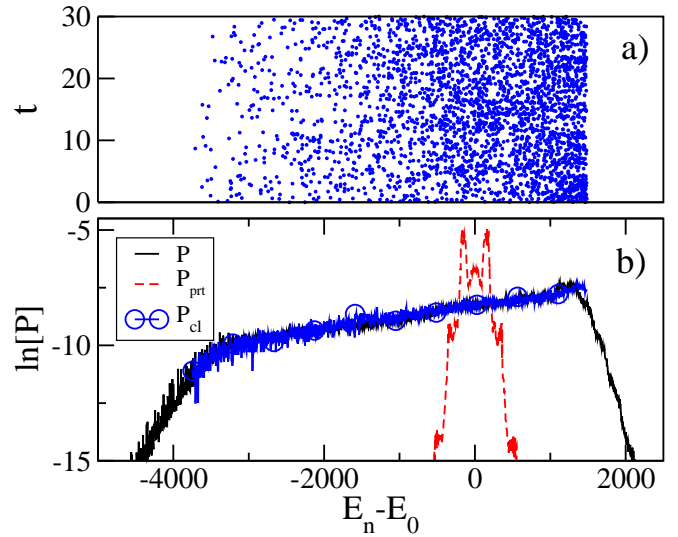


FIG. 4: (Color online) The kernel $P(n|m)$ (LDoS representation) for the BHH in the non-perturbative regime ($\delta k = 10$) for $N = 230$ and $\lambda_0 = 0.053$. In the upper panel we plot a time series $E(t)$ which leads to the classical profile $P_{\text{cl}}(E)$ (see text for details).

- Raghavan *et al.*, *Phys. Rev. A* **59**, 620 (1999).
 [8] J. Reichel, *Appl. Phys. B-Lasers and Optics* **74**, 469 (2002).
 [9] M. Albiez *et al.*, *Phys. Rev. Lett.* **95**, 010402 (2005).
 [10] J. C. Eilbeck, P. S. Lomdahl, A. C. Scott, *Physica D* **16**, 318 (1985); E. Wright *et al.*, *Physica D* **69**, 18 (1993).
 [11] G. P. Tsironis, V. M. Kenkre, *Phys. Lett. A* **127**, 209 (1988); V. M. Kenkre, G. P. Tsironis, *Phys. Rev. B* **35**, 1473 (1987); V. M. Kenkre, D. K. Campbell, *Phys. Rev. B* **34**, R4959 (1986).
 [12] L. Bernstein, J. Eilbeck, A. Scott, *Nonlinearity* **3**, 293 (1990); S. Aubry *et al.*, *Phys. Rev. Lett.* **76**, 1607 (1996).
 [13] G. Kalosakas, A. R. Bishop, V. M. Kenkre, *Phys. Rev. A* **68**, 023602 (2003); G. Kalosakas, A. R. Bishop, *Phys. Rev. A* **65**, 043616 (2002); G. J. Milburn *et al.*, *Phys. Rev. A* **55**, 4318 (1997).
 [14] J. C. Eilbeck, G. P. Tsironis, S. K. Turitsyn, *Physica Scripta* **52**, 386 (1995); D. Hennig *et al.*, *Phys. Rev. E* **51**, 2870 (1995).
 [15] R. Franzosi, V. Penna, *Phys. Rev. A* **65**, 013601 (2002); R. Franzosi, V. Penna, *Phys. Rev. E* **67**, 046227 (2003).
 [16] L. Casetti, M. Pettini, E. G. D. Cohen, *Phys. Rep.* **337**, 237 (2000).
 [17] S. de Filippo, M. Fusco Girard, M. Salerno, *Nonlinearity* **2**, 477 (1989); A. Cheffes, *J. Phys. A* **29**, 4515 (1996); S. Flach, V. Fleurov, *J. Phys.: Cond. Matt.* **9**, 7039 (1997).
 [18] K. Nemoto *et al.*, *Phys. Rev. A* **63**, 013604 (2000).
 [19] A.R. Kolovsky, A. Buchleitner, *Europhys. Lett.* **68**, 632 (2004).
 [20] M. Hiller *et al.*, *Ann. Phys.* **312**, 1025 (2006).
 [21] M. Feingold and A. Peres, *Phys. Rev. A* **34** 591, (1986).
 [22] In our numerical analysis we have defined, δk_{qm} as the perturbation strength for which 50% of the probability remains at the original site, while δk_{prt} is the δk for which the variance of the perturbative expression (6) becomes less than 80% of the exact variance.

- [23] E. Wigner, Ann. Math. **62**, 548 (1955); **65**, 203 (1957); Y. V. Fyodorov, *et al.*, Phys. Rev. Lett. **76**, 1603 (1996).
- [24] D. Cohen and E. J. Heller, Phys. Rev. Lett. **84**, 2841 (2000); A. Barnett, D. Cohen and E.J. Heller, *ibid.* **85**, 1412 (2000); D. Cohen, Ann. Phys. **283**, 175-231 (2000).
- [25] J. A. Méndez-Bermúdez, T. Kottos and D. Cohen, Phys. Rev. E **72**, 027201 (2005); D. Cohen and T. Kottos, Phys. Rev. E **63**, 036203 (2001).
- [26] W. Zwerger, J. Opt. B: Quantum Semiclass. Opt. **5**, S9 (2003).